Journal of Engineering Technology
Volume 6, Issue 1, Jan. 2018, PP. 329-339

RESEARCH ARTICLE -ENGINEERNG TECHNOLOGY

Infrared thermography for the detection of a plaster detachment

Mohamed EL AFI* and Sougrati Belattar
Faculty of Sciences Semlalia, Department of Physics, Marrakech
* Corresponding author

Abstract: Plaster detachment is a pathology that affects traditional mortars, polymeric mortars and ceramic tiles. These anomalies have an effect on the appearance of the concrete structure, facilitate rainwater penetration. Therefore, the reduction of the plaster's durability. In this context, nondestructive techniques are important for inspection purposes. Infrared thermography is one of the suitable techniques of non-destructive evaluation in terms of the detection of the defect in the concrete structure generally and particularly in the habitat system. The main objective of this paper is the analysis of a plaster slab containing two types of delamination, air blades and water blades. The study concerns the effect of the geometry and the size of this delamination. The simulation results by using the finite element method, are presented and analyzed in form of the thermographical images and the temperature distribution.

Keywords: Infrared thermography, Numerical simulation, Non-destructive testing, temperature, blade.

1. Introduction

The search of hidden empty of air or water in a concrete structure in general and in a wall particularly remains a main requirement in the safety and durability of these structures. The weakening of structure caused by the presence of internal detachment of layers is a very serious problem which implies many risks and damages even the breaking of the considered structure. Infrared thermography as one of the effective NDT [1] techniques has proven to be an efficient tool in detecting of hidden detachments [2-4]. The reliability of the infrared thermography method for defect detection makes it as a widely used one for non-destructive evaluation of materials, especially in civil engineering and reinforced concrete for the identification of heat losses in building envelopes or the control of the integrity of concrete structures [5-7].

In this paper, the thermal behaviour of a detachment between a layer concrete and plaster is discussed. The presence of these defects is detected due to a temperature spatial distribution and thermographical images on the structure surface in question. The modelling of different configurations is achieved by using a numerical simulation model based on finite elements modelling (FEM). The model of a parallelepiped concrete structure of concrete and plaster containing cracks in forms of a layer and a spherical form is adopted. This structure is supposed to be excited on the higher face by a heat flux, the lower face being maintained at a constant temperature and the others faces are supposed thermally insulated. The thickness and the position of the crack-layer and the diameter and position of the spherical defect are studied.

2. Description of the model

2.1. Geometrical characteristics of the concrete slab and the defects

To illustrate the application of the TNDT method, the results of the nondestructive testing of a concrete slab of thickness e = 150 mm, L = 1000 mm, and the width L = 1000 mm, where a layer of plaster adhered e = 25 mm, length L = 1000 mm, and the width L = 1000 mm (fig.1), the slab containing 16 equidistant defects in

crack are presented. Defects are parallelepiped and spherical shape.

Lines A_1A_2, A_3A_4, A_5A_6, A_7A_8, B_1B_2, B_3B_4, B_5B_6, B_6B_7, respectivement pass by the point of co-ordinates {(160,160,1) (760,160,1)}, {(160,370,3) (790,370,3)},{(160,580,15) (790,580,15)}, {(160,790,25) (790,790,15)}. {(160,160,1) (160,790,1)}, {(370,160,3), (370,790,3)}, {(580,160,5) (580,790,)}, {(790,160,10) (790,790,10)}.

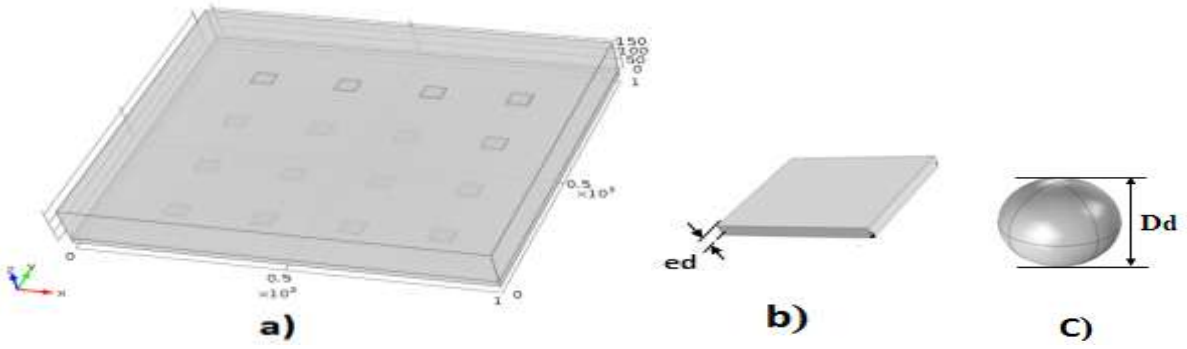

Fig1: a) 3D geometry of the slab, b) Structure of parallelepiped detachment, c) Structure ofspherical detachment

2.1.1 Effect of the volume at constant position

To analyze the effect of the volume parameter, defects were placed at the same position p by report to the input face of plaster according to (-oy) axis and of different volumes ld x ld x edi (ld: the defect side and edi: the variable thickness) for the parallelepiped form fig 2(b), and $\mathbf{kDdi^3}$ (**Ddi**: variable diameter) for the spherical form fig3 (b).

2.1.2. Effect of the position at constant volume

In the same way, to analyze the effect of the position parameter, defects of the same volume were placed at different positions $\mathbf{p_i}$ ($\mathbf{p_i}$: the variable position) by report to the input face of plaster according to (-ox) axis for parallelepiped form, fig 2(e), and spherical form, fig 3(f), forms

a) perspective view b) cutting Ai-Aj axis c) cutting Bi-Bj axis

d) perspective view e) cutting Ai-Aj axis f) cutting Bi-Bj axis

Journal of Engineering Technology
Volume 6, Issue 1, Jan. 2018, PP. 329-339
RESEARCH ARTICLE -ENGINEERNG TECHNOLOGY

Fig 2. Defects of parallelepiped and spherical form

3. Mathematical description of the model

Let us consider the following thermal equation [8-9]:

$$\rho C_p \frac{dT}{dt} - \mathbf{div}\left(\bar{\bar{\lambda}}.\overrightarrow{\mathbf{grad}T}\right) - q = 0 \qquad (1)$$

Where:

ρ : The material density

c_p : The Specific heat capacity

$\bar{\bar{\lambda}}$: The thermal tensor conductivity

q : Voluminal source of heat

With the following boundary conditions:

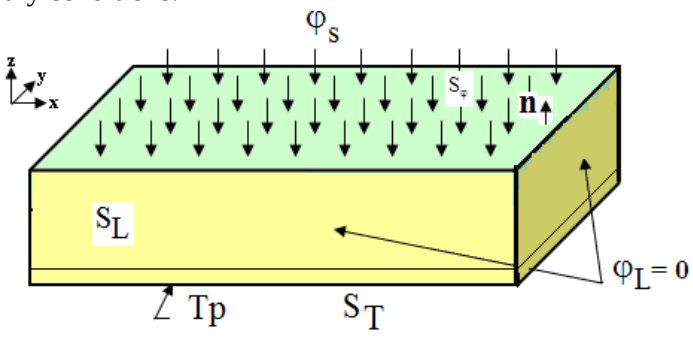

Fig 4

Where: $\mathbf{S_L}$: Side surface

$\boldsymbol{\varphi_L} = 0$: side flow

T_p : The imposed temperature on a surface S_T

φ_S : The imposed flow on the input surface S_φ

$\vec{n}$: The unit vector perpendicular to S and directed towards outside

And the initial condition:

$$T(x,\ y,\ z,\ t_0) = T_0(x,\ y,\ z) \qquad (3)$$

3.1 Numerical modeling

The analytical resolution of the equation (1) is in general inaccessible. Then we look for a solution approached by the finite element method .

The method consists in using an approximation by finite elements of the unknown functions T to discretize the variational form of the equation (1) and to transform it into system of algebric equations of the form [10-12]:

$$[A]\ T = F \qquad (4)$$

Where:

A: is a square matrix of dimension [N_h, N_h]

F: is a vector of N_h components

T: is the vector of the temperatures to be calculated

We start by building the variation form of the equation (1). We carry out a spatial discretization which consists in calculating the elementary integrals by using the finite element and a temporal discretization.
There are many specialized software which make it possible to implement the method of resolution of problems by finite elements in a more or less simple and convivial way. They take care in particular of the grid of the studied object, the automatic numbering of the elements and the nodes, the calculation of a solution then of the chart of the results.
In this study, we used commercial software "Comsol" based on the finite element method which makes it possible to calculate the evolution of temperature at any moment and in any point of material. The material is considered isotropic fig4.

A heat pulse is applied to the upper face of the metal plate, with a flux $\varphi = 50$ w/m^2. The underside of the plate is expected to be maintained at constant temperature Ta = 19°C. The other faces are assumed thermally insulated. The initial temperature of the subdomains is 25 ° C.

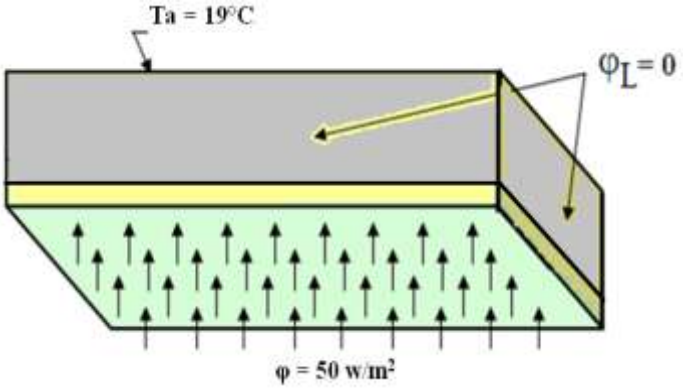

Fig 4: Limit conditions

3.2. Thermophysical characteristics

The table1 shows the thermophysical parameters of metal and defect.

λ : the thermal conductivity (W / m·K)
ρ : represents the density of the material (kg/m^3)
C_p: represents the heat capacity at constant pressure (J / kg.K)

Table1. Thermophysical parameters

Materials	thermal conductivity [W/ (m*K)]	Density of the material [kg/m3]	heat capacity at constant pressure [J/ (kg*K)]
Concrete	1.8	2300	385
Plaster	0.35	950	1000
Plâtre à 20 C	0.8	830	1600

Air	0.0272	1.1845	100
Water	0.589	999.045	4180

4. Simulation results

4.1. Effects of the defect thickness and position

In this section, we are inserted defects of parallelepiped form, fig5 (a) and of spherical form fig5(c) in a concrete slab, having successively (along the y axis increasing) the thickness e_d = 1mm, 3mm, 5mm and 10mm for the parallelepiped and the diameter D_d =16.84mm, 24.28mm, 28.80 mm and 36.28 mm for the spherical forms. Each of these thickness and these diameters were placed at for different positions: p =1 mm, 3 mm, 15 mm and 25 mm from the input face.

Fig.5 (b) shows the thermographical image of concrete slab subjected to a step of heat flow in steady mode. The related images to parallelepiped or spherical forms clearly show the colors contrast representing different levels the sample surface temperature. The contrast amplitude depends on the volume and the location of the defect in the structure. Through these thermal images one can note that the defect effect is much larger when it is close to the input surface or of a larger volume. On the thermal images, fig5, thermal spots reproduce the shape of the internal defect. The form of the task is related to the form of the internal defect.

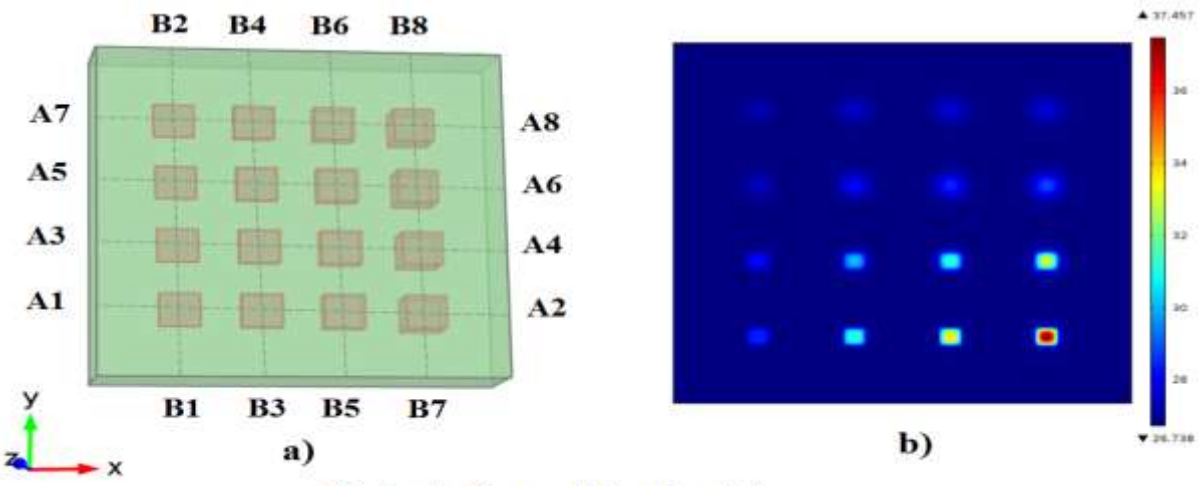

Defect of parallelepiped form

Journal of Engineering Technology
Volume 6, Issue 1, Jan. 2018, PP. 329-339
RESEARCH ARTICLE -ENGINEERNG TECHNOLOGY

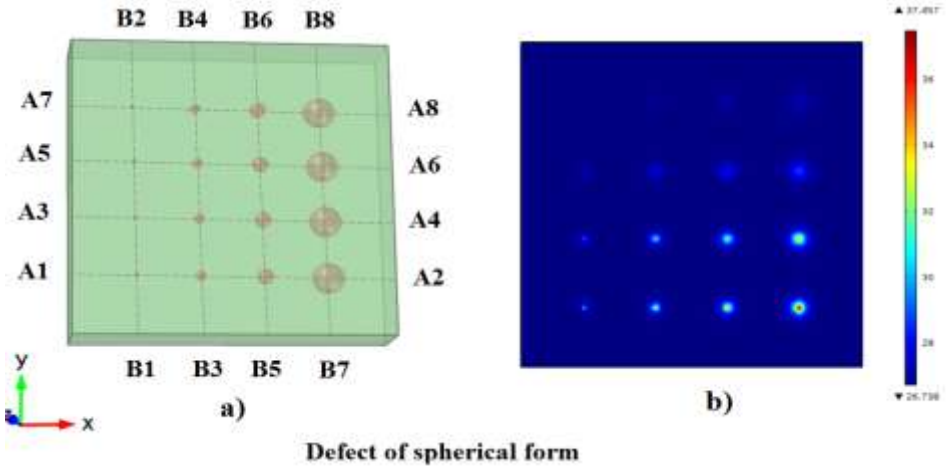

Fig.5: distribution of cracks in concrete slab (a) and thermographical images (b)

4.1.1 Thickness or diameter effect for a constant position

The fig6 represents the surface temperature spatial evolution of the input concrete slab. At a constant position, the defect effect depends on the thickness or diameter of the defect for each position respectively of the crack or the air pocket.

Analysis according to A2 - A1 axis, where the defect position is constant and the volume is variable. We can note from the images of figs (5b) that according to each axis among A_1-A_2, A_3-A_4, A_5-A_6 or A_8-A_7 axis, defects are in the same position by report to the sample input surface and that the defect who has the largest volume, it is the one who creates the greatest temperature disturbance on the sample surface. More the defect volume increases more the peak amplitude of the sample surface spatial temperature increases and therefore it is the greatest stain on the thermographical image. This means that, at constant position, when the volume of the crack is large, the easier it is to detect, and vice versa. This phenomenon is observed for both types of defects.

On the thermographical image, the size of the stain created by the defect is related to the effective defect surface seen from the input surface of the structure (projection of the defect on the input surface). The results show that for a spherical defect which has an area surface equivalent to a circular area of radius D_d / 2. So the corresponding stain is small compared to that of a square surface as in the parallelepiped form which makes this relatively simple to detect for small dimensions of defect.

Journal of Engineering Technology
Volume 6, Issue 1, Jan. 2018, PP. 329-339

RESEARCH ARTICLE -ENGINEERNG TECHNOLOGY

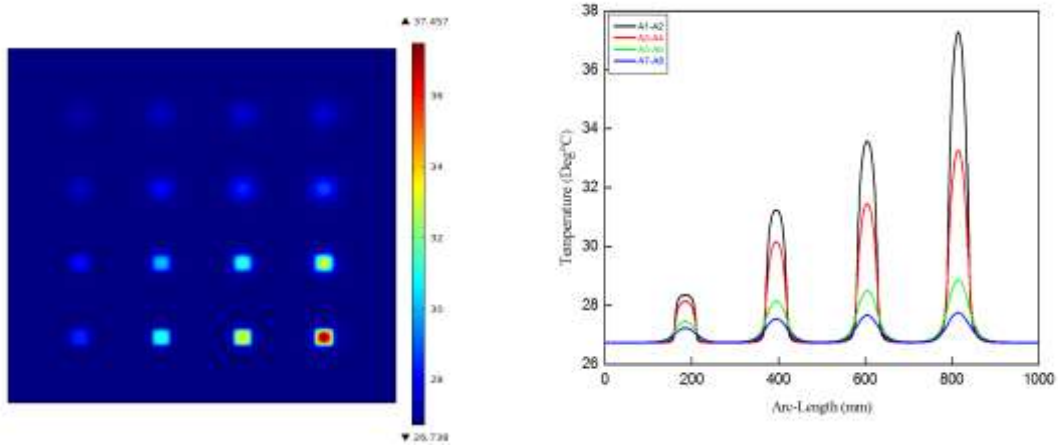

Ai-Aj	P = 25mm	P = 15mm	P = 5mm	P = 1mm
A1-A2	28.40	31.30	33.70	37.47
A3-A4	28.20	30.25	31.50	33.50
A5-A6	27.48	28.20	28.50	28.90
A7-A8	27.25	27.56	27.68	27.80

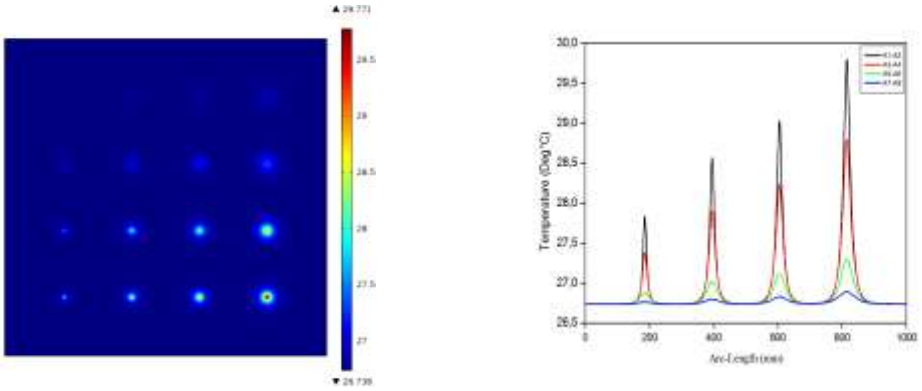

Ai-Aj	P = 25mm	P = 15mm	P = 5mm	P = 1mm
A1-A2	27.80	28.60	29.00	29.80
A3-A4	27.40	27.90	28.20	28.80
A5-A6	26.88	27.02	27.12	27.30

A7-A8	26.76	26.80	26.83	26.89

Fig6. Effect of the crack thickness (volume), for the parallelepiped form (a) and the effect of diameter of spherical form (b), on the surface temperature profile of the aluminum plate for four defect positions, p= 1 mm; 4mm; 7.5 mm and 11 mm.

4.1.2 Position effect for a constant volume

Analysis according to B2-B1 axis, where the defect volume is constant and the defect position is variable. The analysis of curves along the axis B2-B1, B4-B3, B6-B5 or B8-B7 illustrates the importance of the defect position in the metal structure. In fact, ranging from the farthest defect position by report to the input surface of the sample (from B2 to B1, taking the volume as constant) to the closest one, the peak value of the temperature increases and vice versa. The same phenomenon is observed on the axis B4 - B2 ... etc.. These results show that, for a given volume, the value of the peak temperature is related to the position of the defect in the structure. Again we can conclude that, at constant volume, when the crack is the more close to the sample input surface the more easier it is to detect and vice versa.

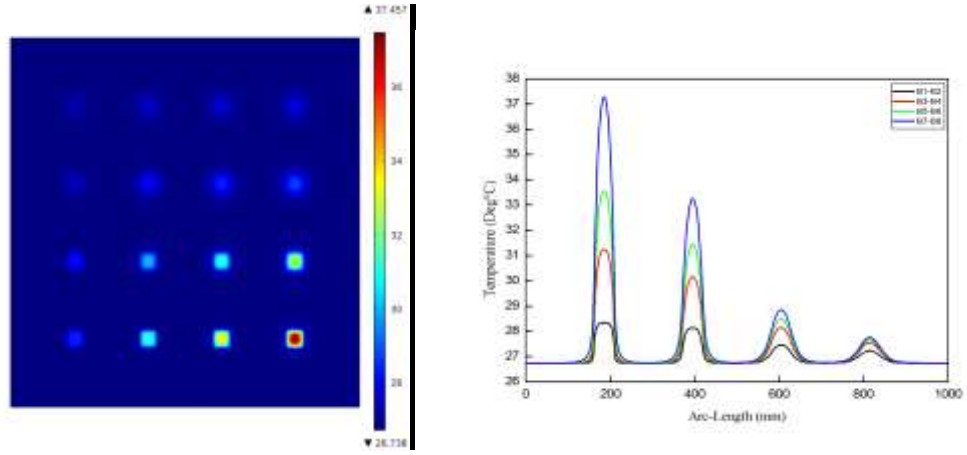

(a). Effect of the crack position on the surface temperature profile of the aluminum plate for four different value of crack thickness ed= 1 mm; 3 mm; 5 mm and 10 mm

Bi-Bj	ed = 10mm	ed = 5mm	ed = 3mm	ed = 1mm
B7-B8	37.28	33.25	28.90	27.75
B5-B6	33.50	31.50	28.50	27.70
B3-B4	31.50	30.20	28.20	27.50
B1-B2	28.35	28.15	27.46	27.24

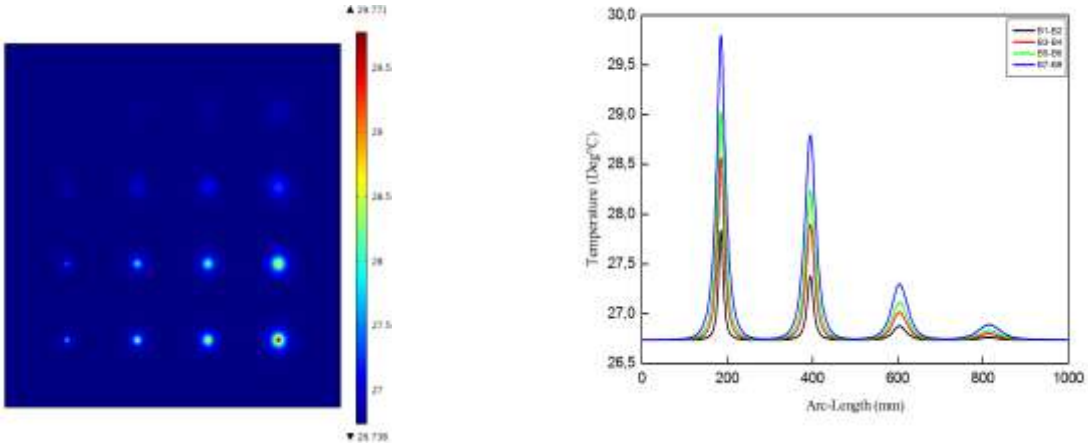

Bi-Bj	ed = 10mm	ed = 5mm	ed = 3mm	ed = 1mm
B7-B8	29.80	28.80	27.30	26.90
B5-B6	29.00	28.20	27.10	26.84
B3-B4	28.60	27.90	27.02	26.80
B1-B2	27.85	27.38	26.88	26.75

(b) Effect of the air bubble position on the surface temperature profile of the aluminum plate for four different value of diameters Dd= 1 mm; 3 mm; 5 mm and 10 mm
Fig 7 Effect of the defect position in the aluminum plate

4.1.3 Effect of the thermophysical nature of defect

In this section we sought to know what will be the behavior of the system when the thermophysical characteristics of defect changes. To see what about the detectability of these defects in air compared to others known like water we performed simulations presented in Fig (8) and (9). In these simulations, the same geometry of system is taken for the two cases.

Fig 8. Effect according to Ai-Aj Axis of the crack thickness(a) for parallelepiped form and of the defect diameter (b) for spherical form, on the surface temperature profile of the plate, for three materials :aluminum, copper and steel and for four positions p=1mm , 4 mm, 7.5 mm and 11 mm.

According to the curves of fig 8, the average surface temperature of the aluminum plate is very close to that of copper at 0.05 ° C accuracy. By cons is not negligible when it comes to steel. In fact the difference between the average of surface temperature aluminum and the steel one is approximately 0.2 ° C. It appears from these results that the presence of anomalies such as cracks or air bubbles is relatively easier to detect in the less conductive metals such as the steel compared to aluminum or copper. These two metals, aluminum and cooper, are highly conductive and tend to equalize the surface temperature and consequently to minimize the temperature contrast which makes difficult an eventual anomalies detection for low temperatures.

Journal of Engineering Technology
Volume 6, Issue 1, Jan. 2018, PP. 329-339
RESEARCH ARTICLE -ENGINEERNG TECHNOLOGY

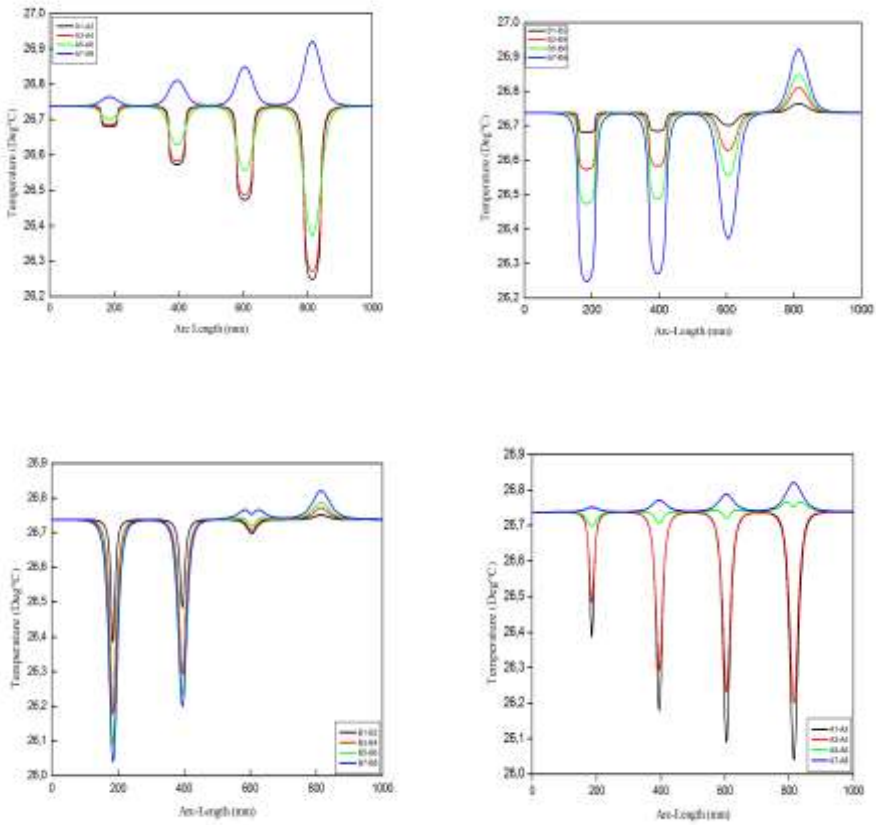

Fig 9. Effect according to Bi-Bj Axis of the position of the crack **a):** parallelepiped form and b**):** spherical form, on the surface temperature profile of the plate, for three materials: aluminum, copper and steel and for four thickness for **a):** parallelepiped form, ed = 1 mm, 3 mm, 5 mm and 10 mm and the diameter **b):** spherical form Dd = 1 mm, 3 mm, 5 mm and 10 mm.

The same phenomena of the previous section are observed on the curves of Fig 9 when it comes to analyzing the evolution according the Bi-Bj axis.

5. Conclusion

The numerical simulation performed prove that detachments are easy to detect, as they produce an air layer between the plaster and masonry, introducing additional thermal resistance and altering the distribution of temperature of the areas with anomalies. it was possible to detect detachments in samples, using a heat source. All the detachments analyzed produced higher temperatures than the plaster without defects during exposure to a heat source. Without the action of a heat source, during the cooling phase, the temperatures were lower in the detachment. This study shows that thermography is a useful tool for the nondestructive diagnosis of the plaster detachment, and may facilitate early detection.

References

[1] Capozzoli, Luigi, and Enzo Rizzo. "Combined NDT techniques in civil engineering applications: Laboratory and real test." Construction and Building Materials 154, pp: 1139-1150, 2017.

[2] Maldague Xavier and Marinetti Sergio, « Pulse phase infrared thermography", Journal of applied physics, vol(79)5, pp=2694:2698, 1996.

[3] Clark, MR and McCann, DM and Forde, MC," Application of infrared thermography to the non-destructive testing of concrete and masonry bridges", journal Ndt & E International ,vol.(36)4, pp: 265:275, 2003.

[4] Maldague, Xavier PV. Nondestructive evaluation of materials by infrared thermography. Springer Science & Business Media, 2012.

[5] Tran, Quang Huy, et al. "Effects of Ambient Temperature and Relative Humidity on Subsurface Defect Detection in Concrete Structures by Active Thermal Imaging." Sensors 17.8 (2017): 1718.

[6] Hiasa, Shuhei, Recep Birgul, and F. Necati Catbas. "Effect of defect size on subsurface defect detectability and defect depth estimation for concrete structures by infrared thermography." Journal of Nondestructive Evaluation 36.3 (2017): 57.

[7] Hussain, Aslam, and Saleem Akhtar. "Review of Non-Destructive Tests for Evaluation of Historic Masonry and Concrete Structures." Arabian Journal for Science and Engineering 42.3 (2017): 925-940.

[8] A. Elballouti, S. Belattar, A. Obbadi. S. Sahnoun "Numerical method applied to the non-destructive characterization of the cracks in the roadways" 12th A-PCNDT 2006 – Asia-Pacific Conference on NDT, 5^{th}– 10^{th} Nov 2006, Auckland, New Zealand.

[9] A; Elballouti, S. Belattar: "Numerical method applied to the non-destructive characterization of the cracks in throadways" Physical & Chemical News 35 (May 2007) 43-47.

[10] J.Rhazi, S.Naar Aptitude de la thermographie infrarouge à détecter les fissures et les nids d'abeille dans le béton", 12ème colloque sur la progression de la recherche québécoise sur les ouvrages d'art (2005).

[11] S.Maillard, J.Cadith, H.Walszek, A.Dillenz « La thermographie infrarouge stimulée, une nouvelle technique de contrôle sur les lignes de production », Cofrend 2008 Toulouse, 20 – 23 mai, 2008

[12] S.Belattar, S.Sahnoun "Thermal nondestructive testing study of a circular defect in plane structure 8th ECNDT European Conference on Nondestructive Testing Barcelona (Spain), June 17-21, 2002.